

Mantle anisotropy in NW Namibia from XKS splitting: asthenospheric flow, magmatic underplating, and lithospheric shearing

Abolfazl Komeazi¹, Ayoub Kaviani¹, Georg Rümpker^{1,2}

1. Institute of Geosciences, Goethe-University Frankfurt, Frankfurt, Germany

2. Frankfurt Institute for Advanced Studies, Frankfurt, Germany

Abstract

The presence of the Etendeka flood basalts in northwestern Namibia is taken as evidence for the activity of the Tristan da Cunha mantle plume during the breakup process between Africa and South America. We investigate seismic anisotropy beneath NW Namibia by splitting analysis of core-refracted teleseismic shear waves (XKS phases) to probe mantle flow and lithospheric deformation related to the tectonic history of the region. The waveform data were obtained from 34 onshore stations and 12 Ocean Bottom Seismometers.

The results presented here are from joint splitting analysis of multiple XKS phases. The majority of the fast polarization directions (FPDs) exhibit an NE-SW orientation consistent with a model of large-scale mantle flow due to the NE motion of the African plate. No evidence for a direct effect of the mantle plume is observed. In the northern part, we observe NNW-SSE oriented FPDs that is likely caused by shallow lithospheric structures.

Key Points

- Seismic anisotropy in the upper mantle beneath NW Namibia is mainly due to the absolute motion of the African Plate.
- No significant direct effect of the mantle plume is observed in shear wave splitting measurements.
- Localized shearing in the lithosphere and crustal underplating are likely the main causes of the lateral variations in seismic anisotropy.

Plain Language Summary

The geology of North-west Namibia is characterized by the presence of flood basalts, originated from magma sourced in the mantle. The source magma of these flood basalts was produced during the passage of the African plate over a mantle plume at ~80-90 million years ago, contemporaneous with the onset of breakup of the South American plate from the African plate. The role of the mantle plume in the continental breakup can be examined using our tool, shear wave splitting. It allows examining the flow of material below a region by analysis of seismic waves traveling through the mantle. The mantle flow induces direction-dependent physical properties, called anisotropy, which causes a shear seismic wave to split into two different components travelling at different speeds. The leading component is polarized in a direction representing the direction of the flow in the earth. Except for the northern part, the polarization direction of the fast shear wave is consistent with the model of mantle flow that is caused by the NE motion of the African plate. The results of our study suggest that the mantle plume had indirect impact on the mantle beneath our region of study.

1 Introduction

The opening of the South Atlantic oceanic basin is considered a classical example of a mantle plume-related continental breakup. The occurrence of the Paraná-Etendeka conjugate continental flood basalt (CFB) provinces (now in Uruguay and NW Namibia) is often assumed as evidence for the onset of the Gondwana breakup at ca. 130 Ma (Renne et al., 1992; Wilson, 1992; Renne et al., 1996). However, the role of mantle plume-plate interaction in the continental breakup and opening of the South Atlantic Ocean is still under debate. There are also several theories about the cause of the massive basaltic extrusions, including the idea of a mantle plume whose surface expression can be correlated with the present-day hotspot on Tristan da Cunha (TdC) in the South Atlantic Ocean (e.g. Heine et al., 2013; Fromm et al., 2017a,b). The analysis of shear wave splitting to infer the pattern of mantle flow and mantle deformation provides a powerful tool to examine the hypothesized plume-plate interaction (e.g. Ito et al., 2014).

1 Our study is focused on the eastern coast of the South Atlantic Ocean and NW Namibia and
2 includes parts of the Congo and Kalahari Proterozoic cratons as well as the Damara belt that
3 separates the cratons and the coast-parallel Kaoko belt (Fig. 1). At about 550 Ma, the Damara
4 belt was developed in the Congo-Kalahari craton as evidenced by deformed Neoproterozoic
5 rocks exposed in the Kaoko belt, as one of the coastal arms of the Damara orogen (Begg et al.,
6 2009). The Kaoko belt formed ~600 Ma and represents the northern coastal arm of a triple
7 junction within the Pan-African Orogenic System (Begg et al., 2009). There are two major
8 structural units in the Kaoko belt: the Puros Shear Zone and the Sesfontein Thrust, which divide
9 it into three different tectonic units.

10
11 The upper mantle structures beneath the study region have been explored over the last two
12 decades by a number of seismological investigations (e.g., Moulin et al. 2010; Ussami et al.
13 2013; Ryberg et al. 2015; Yuan et al. 2017; Hu et al. 2018; Celli et al. 2020). Several surface-
14 wave tomography studies have explored azimuthal anisotropy (e.g. Hadiouche et al. 1989).
15 Seismic tomography studies (e.g. Wilson, 1992; De Wit et al. 2008; Hu et al., 2018; Celli et al.,
16 2020; Pandey et al., 2022) suggest that the deep lithospheric root beneath the western margins of
17 the Congo and Kalahari cratons was eroded and delaminated by a mantle plume during the Late
18 Cretaceous and early Cenozoic. Some other studies, including Gibson et al., (2005), support the
19 idea that the occurrence of the CFB provinces as well as the development of the Walvis Ridge
20 (WR) is related to the activities of a mantle plume. Heit et al. (2015) found a relatively thick
21 crust (up to 45 km) at the intersection of the WR and African continent. This crustal thickening
22 was interpreted as evidence of magmatic underplating at the base of the crust induced by plume
23 activity. Using P and S receiver function data, Yuan et al. (2017) found that the region may have
24 experienced underplating or plume melting, resulting in a highly melt-depleted, dehydrated
25 boundary layer.

26
27 Long-term deformation and flow in the mantle may leave a record of seismic anisotropy in the
28 mantle and crustal rocks (e.g. Savage, 1999; Long & Silver, 2009). The main cause of seismic
29 anisotropy in the upper mantle is the lattice-preferred orientation (LPO) of rock-forming
30 minerals especially olivine (Nicolas & Christensen 1987; Mainprice et al. 2000). Seismic
31 anisotropy can be caused by lithospheric deformation acquired and frozen-in during past tectonic

processes (Silver 1996; Barruol et al. 1998) beneath regions that underwent significant deformation processes (e.g., orogenic belts, extensional domains, and shear zones).

The study of seismic anisotropy, therefore, can help to address general questions relevant to the plume-lithosphere interaction. Splitting analysis of core-refracted teleseismic shear phases (such as SKS and PKS named XKS henceforth) is a well-known approach to investigate seismic anisotropy in the mantle (e.g. Silver & Chan, 1991). As a result of the P-to-S conversion at the core-mantle boundary (CMB), XKS phases are polarized in the radial direction and loose the effects of source-side anisotropy. In a shear-wave splitting analysis two parameters, the polarization direction, ϕ , of the faster component of the split shear wave and the delay time, δt , between the two quasi-shear waves, are measured as a proxy for the orientation and strength of seismic anisotropy beneath a seismic station.

In this study, we perform splitting analysis on XKS waveform data collected from 46 broad-band stations (34 land stations and 12 offshore OBS stations) to study seismic anisotropy in NW Namibia. The offshore OBS stations cover the eastern part of the Walvis Ridge in the Atlantic Ocean. The goal of our study is to investigate the relationship between the surface structures generated by main tectonic events and internal lithospheric deformation and mantle flow. The main tectonic events to be considered include the Proterozoic continental accretion and the interaction between the Tristan da Cunha plume and the African plate and its relationship with the continental breakup and ocean rifting process since the Late Cretaceous.

2 Method and results

2.1 Data sets

We analyzed XKS waveform data from two seismic networks XC (Kind, 2000) and 6A (Heit et al., 2010), and a permanent global station. The network XC, consisting of 5 stations and operated from February 1998 to November 1999, was deployed to investigate the role of the mantle plume in an active continental margin. Network 6A, also known as WALPASS (Walvis Ridge Passive

Source Experiment), consists of 28 onshore stations in Namibia's northwestern region (operated between October 2010 and November 2012) and 12 offshore (OBS) stations (operated between January 2011 and January 2012). The network was installed to examine potential seismic anomalies related to the postulated hotspot track that extends from the continent to the ocean along the Walvis Ridge and to constrain the lithospheric and upper mantle structure beneath the passive continental margin of northern Namibia (Heit et al., 2010).

2.2 *Shear-wave splitting analysis*

XKS waveform data were collected from teleseismic events in the epicentral distance range 85° - 140° (Fig. 1) and with magnitudes $M_w > 6.0$, which provided a total number of ~2450 seismograms from 457 events. The splitting analysis was performed using the SplitRacer code (Reiss & Rumpker, 2017). The origin time and location of the teleseismic events were taken from the National Earthquake Information Center (NEIC). The theoretical arrival times of XKS phases are calculated based on the IASP91 reference model to determine the time window for splitting analysis. Seismograms are generally filtered between 0.02 Hz and 0.2 Hz in order to eliminate long-period and high-frequency noise that might interfere with the XKS waveform. Three steps are involved in pre-processing of the waveform dataset: i) initial screening where the filtered XKS waveforms are selected based on their signal-to-noise ratio, ii) visual quality check: only phases that meet the previous criteria are displayed and by visual inspection, only phases suitable for splitting analysis are kept (based on the sharpness of the waveform and the shape of the particle motion), iii) we check for possible misalignment of the sensors based on the difference between the theoretical backazimuth and the azimuth of the principle axis of the long-period elliptical particle motion. In the case of misalignment of a sensor, the horizontal seismograms are rotated to the correct azimuth before splitting analysis. We also have the option to manually choose a time window over which the XKS phase is captured correctly with less interference from other phases. There are some factors such as the aspect ratio of the elliptical particle motion to help us with selection.

Following the first step of pre-processing and selection, single measurements are computed from individual XKS phases based on the transverse component energy minimization approach (Silver

& Chan, 1991). For a selected time window, the splitting parameters ϕ and δt are determined so that energy on the transverse component of the seismogram is most effectively reduced. The main goal of the single-phase analysis is to verify the suitability of each phase for the final joint inversion of multiple phases observed at a single station. Furthermore, the azimuthal variations of the single measurements at each station provide a first indication of the complexity of the anisotropic structure beneath the station. The single measurements are considered reliable if the horizontal fast-and slow-component waveforms are coherent, and the initial particle motion is elliptical and becomes linear after correction for anisotropy (Silver & Chan, 1991). The SplitRacer code allows selecting an initial time window encompassing the phase under analysis. It then automatically chooses a number of alternative time windows (up to 10 windows here), with start and end values are randomly distributed around corresponding values for the initial window. Splitting analysis is then performed for all the selected time windows and the average value of the splitting parameters is reported as the single measurement for the selected phase. SplitRacer also enables categorizing the single splitting measurements by assigning quality such as good, average, and poor to each measurement. This is done manually based on the elliptical shape of the particle motion, the percentage of reduction in energy on the transverse component, the size and form of the 95% confidence contour, the distribution of ϕ and δt values from different chosen time windows, and the correlation between fast and slow split shear waves components. Two examples of the categorized measurements are shown in Fig S1. Some measurements are also categorized as “null” based on the linearity of the uncorrected particle motion and reduction of T-component energy. A null measurement is obtained from a non-split waveform when either there is no anisotropy beneath the station, or the initial polarization direction of the wave is parallel to either the fast or slow direction in the anisotropic layer.

Finally, phases corresponding to good and average single measurements are selected for the joint splitting analysis at each station. The joint splitting analysis inverts all qualified waveforms at a given station, including those phases giving null measurements. In this approach, a grid search is applied to find two splitting parameters (ϕ and δt , equivalent to the anisotropic parameters of a 1-layer model) that simultaneously minimize the total energy of all the T-component waveforms at the station. The correction of the T-component waveforms for anisotropic parameters is performed using an inverse splitting operator (Rümpker & Silver, 1998).

2.3 Results

The results of the single-phase splitting measurements are shown on the map at station locations in Fig. 2a. Red bars in this figure indicate fast polarization directions (FPDs) with lengths proportional to the associated delay times. The black arrows show back-azimuth of events giving null measurements. We obtained considerable reliable measurements at land stations, though the offshore stations give relatively less measurements. We observe consistent non-null measurements with some azimuthal variations in the splitting parameters at a number of stations. The majority of single measurements at the land stations orient in an NE-SW direction. We also obtained null measurements (black arrows) with back-azimuths mainly either parallel or perpendicular to the fast directions. These observations suggest the presence of a simple anisotropic structure overall beneath the region. However, we also observe azimuthally varying measurements at a few stations. For example, at station TSUM with more than two decades of data, we obtained relatively small delay times and many null measurements.

Variations of splitting parameters (φ and δt) with respect to back-azimuth and incidence angle may indicate layered anisotropy or more complex structures (e.g. Silver & Savage, 1994; Rumpker & Silver, 1998; Hartog & Schwartz, 2000). In the case of depth-dependent anisotropy, φ and δt are expected to exhibit a $\pi/2$ periodicity as function of back-azimuth. Examples of the variation of the single splitting parameters as a function of the event back-azimuths are shown in Fig. S2, at stations with more than 10 reliable measurements. We tried to invert the splitting parameters for 2-layer anisotropic models at stations with sufficient back-azimuthal coverage. Examples of the 2-layer modeling for stations WP01 and TSUM are shown in Figs S3c and S3d. Our analysis suggests that the 2-layer models cannot explain the data better than 1-layer models (Figs S3a and S3b). Similar results are obtained for other stations suggesting that the assumption of a 1-layer anisotropic model beneath the most part of the study area is valid within the range of the azimuthal coverage of our dataset. We argue that the variation of splitting parameters at stations such as TSUM can be due to local 3-D heterogeneities (e.g. Vauchez et al. 2000) rather than a simple 2-layer model with horizontal symmetry axes.

Following the analysis of the single measurements, we concluded that the assumption of 1-layer models beneath the stations is valid in the study area. Therefore, we jointly analyze the XKS phases of each station to obtain average splitting parameters representative of the 1-layer models. The 1-layer model parameters for all stations obtained by the joint analysis are shown in Fig. 2b and Table S1 (supplementary materials). Table S1 also shows that the amount of useful phases varies for each station. No reliable joint analysis measurements could be obtained at 5 OBS stations (WPO 03, 07, 08, 09, and 12) and from the land station BRAN (Fig. 1) due to the relatively low signal-to-noise ratio of the XKS waveforms. We observe a consistent NE-SW trend of the single layer fast directions at the majority of the stations. On the other hand, we see an anticlockwise rotation of the fast directions from the dominantly NE-SW direction in the SW region to an NNW-SSE direction in the NW region of the study area. The possible scenarios for this lateral variation in the fast directions are discussed in the next section.

3 Discussion

One objective of this study is to examine the plume-plate interaction in a region where the emplacement of extensive continental flood basalt is thought to mark the onset of the opening of the South Atlantic Ocean in the Cretaceous. The track of the potential mantle plume can be traced from NW Namibia over the Walvis Ridge to the present-day hotspot on Tristan da Cunha (TdC) (Richards et al., 1989). The results of the XKS splitting analysis presented in this study show a relatively uniform pattern with local small-scale variations in the splitting parameters. We discuss these results in a broader context of the African plate motion and possible scenarios regarding how the mantle plume and local structures could have left signatures in terms of seismic anisotropy.

3.1 Plate motion induced mantle flow

In order to consider the XKS splitting pattern in a broader context in western Africa, we show in Fig. 3 our results (red bars) alongside measurements (blue bars) from previous studies (Barruol, et al. 2009). The fast polarization generally trend NE-SW, in agreement with previous studies.

1 Also, our measurements of joint splitting parameters at station TSUM agree well with previously
2 reported results (Barruol & Ismail, 2001), with a minor differences in ϕ (6°) and δt (0.2 sec).

3
4 The relatively coherent and predominantly NE-SW-oriented pattern of the observed FPD in
5 western Africa is subparallel to the absolute plate motion indicated with the black arrows in Fig 3
6 in the No-Net-Rotation reference frame (Kreemer, et al., 2014). These observations suggest that
7 the main cause of the underlying anisotropy is likely the large-scale mantle flow due to the
8 motion of the African plate relative to the underlying asthenosphere. This uniform pattern of
9 anisotropy is locally perturbed, which could be an effect of locally modified mantle flow or
10 related to shear zones in the overlying lithosphere.

11 12 *3.2 Large scale mantle-plume signature?*

13
14 One process responsible for the pattern of mantle flow beneath the NW Namibia is the effect of
15 an impinging mantle plume. Previous studies suggest that a mantle plume was active beneath the
16 region during the continental breakup, even likely emplaced before the onset of the breakup (e.g.,
17 Brune et al., 2013; Heine et al., 2013; Brune et al., 2016). However, the lateral extent of the
18 affected area by the mantle plume beneath the region is not clearly known. Fromm et al. (2015
19 and 2017a) using seismic refraction data identified structures suggesting that no broad plume
20 head existed during the opening of the South Atlantic that could modify the continental crust on
21 a large scale. They also suggest that anomalous mantle melting may have occurred only locally.

22
23 A mantle plume can produce a parabolic or radial asthenospheric flow depending on the relative
24 motion between the lithospheric plate and underlying asthenosphere (e.g., Walker et al., 2001;
25 Druken et al., 2013; Ito et al., 2014). The complex pattern of seismic anisotropy in active hot
26 spot regions reflects the signature of mantle plumes (e.g. Walker et al., 2005; Collins et al., 2012;
27 Barruol & Fontaine, 2013; Ito et al., 2015). The XKS splitting measurements in our study,
28 however, do not exhibit a radially oriented pattern that would reflect the effect or track of a
29 plume head. One possible scenario is that the plume head was very broad extending beyond the
30 aperture of our seismic network such that the associated flow pattern could not be detected by
31 our observations. In the case of a limited extent of the mantle plume head, we argue that either

no coherent anisotropic fabric was developed by the flow related to the plume head or the possible fabric was reworked by later phases of continental breakup and plate motion. Seismic tomography models (e.g. Hu et al., 2018; Celli et al., 2020; Pandey et al., 2022) suggest the lower part of the lithosphere was eroded and delaminated by the mantle plume in the Cretaceous. The thickness of the lithosphere was later resumed by cooling of the plume melts and accretion of the depleted lithospheric segments. These lithospheric removal and reconstruction processes could have erased the potential fabric originally generated by the mantle plume.

3.3 Underplating and lithospheric shearing

The splitting parameters of the 1-layer anisotropic model beneath each station are depicted in Fig. 2a overlapped on the main geological units including the Kaoko and Damara belts, the Puros shear zone, and the Kalahari and Congo cratons. We clearly see a dominantly NNW-SSE trend of FPD at the majority of the stations located in the Kaoko, exhibiting an anticlockwise rotation relative to the general NE-SW trend of the FPD in western Africa. Considering this small-scale variation in the FPDs and the fact that the average values of δt for all the stations are below one second, we conclude that this pattern in splitting parameters is related to the lithospheric anisotropy sources. By considering the Fresnel-zone width (Rümpker & Ryberg, 2000) at close stations (WP12 and WP27) exhibiting different anisotropy directions, we estimate that the lateral change in the anisotropic structure occurs at depths between 30 and 60 km, by considering 35% and 45%, respectively, of overlap of Fresnel zones at nearby stations. We, therefore, attribute the NNW-SSE trending seismic anisotropy in NW Namibia to the effect of the tectonic evolution of the lithosphere, including the formation and evolution of the Kaoko and Damara orogenic belts and the breakup of the continental plate in late Cretaceous.

Ryberg et al. (2015) identified a narrow region of high seismic velocity anomalies in the middle-lower crust and interpreted them as a mafic intrusion into the northern Namibian continental crust. A study by Planert et al. (2017) argues that rift-related lithospheric stretching and associated transform faulting can play a major role in locating magmatism. Coast-parallel faults that likely penetrate down to the base of the lower crust (Foster et al., 2009; Fromm et al., 2015) also indicate a zone of stretching that could have facilitated magma intrusion beneath the crust.

1 Therefore, we surmise that in the absence of a large plume head, an indirect plume-induced
2 anisotropy in the form of shape-preferred orientation (SPO) fabric developed during crustal
3 underplating beneath NW Namibia can explain the observation of the NNW-SSE trending FPDs.
4

5 One other factor that should be considered is the fabric left in the crust and shallow mantle from
6 the Neoproterozoic tectonic activities. Based on the coincidence between the strike of the
7 Neoproterozoic structures at the surface and the NNW-SSE orientation of our FPDs at the
8 stations located above the Kaoko belt, we argue that the processes developing the belt could also
9 have left some coherent anisotropic fabric at depth. According to Goscombe et al. (2003), the
10 Kaoko belt has evolved in different phases. Following an early thermal phase that resulted in
11 pervasive partial melting and granite emplacement in the western zone (656 Ma), a
12 transpressional phase shaped the geometry of the belt (580-550 Ma). Strain partitioning in the
13 Puros shear zone and the NE-SW oriented shortening in the Central zone supports a sinistral
14 transpressional movement in the second phase, followed by a minor NNW-SSE shortening (530-
15 510 Ma). Due to the extensive and large-scale nature of these Precambrian tectonic processes,
16 which could also have affected the upper mantle beneath the Kaoko belt, they could have
17 produced a pervasive NNW-SSE oriented anisotropic fabric sub-parallel to the strike of the
18 Puros shear zone.
19
20

21 **Conclusion**

22

23 We present new results of the upper mantle seismic anisotropy beneath NW Namibia. From XKS
24 splitting analysis we detect seismic anisotropy at the majority of the 45 land and OBS stations
25 used in this study. The measurements generally suggest that the upper mantle structure beneath
26 the study area is consistent with the general trend of the absolute motion of the African plate in
27 the No-Net-Rotation reference frame, except for stations located above the Kaoko belt. Based on
28 our XKS splitting analysis, we argue that the Tristan da Cunha mantle plume had a passive and
29 secondary role during the Cretaceous continental breakup in western Africa. Our results indicate
30 that the plume did not produce an extensive lateral flow to develop a pervasive fabric in the
31 mantle. A possible minor effect of the mantle plume was likely overprinted by later processes

during the Cenozoic that have led to the resumption of the thickness of the lithosphere. The NNW-SSE trending FPDs in the NW part of our study area likely reflect anisotropic fabric developed in the crust and uppermost mantle by the superposition effect of two main tectonic processes. One is the underplating and emplacement of melt pockets within cracks in the uppermost mantle and at the base of the crust, developing an SPO anisotropic fabric. The other is the Neoproterozoic orogeny and shearing in the Kaoko belt, which affected the entire thickness of the lithosphere and was able to develop strike-parallel anisotropic fabric.

Figure Captions

Figure 1. Map showing the study area and the location of seismic stations used in this study. Red triangles denote the network 6A (WALPASS) land stations and black triangles denote the off-shore stations from the same network. The blue triangles represent stations of network XC. The single permanent station in the region, TSUM, is shown by the yellow triangle. Black thick lines approximately mark the boundaries of the Congo and Kalahari cratons. Dark gray areas depict the northern and southern Etendeka flood basalts (modified after Yuan et al. 2017). The inset map at the bottom left shows the current position of the Tristan da Cunha (TdC) hotspot, and the Walvis Ridge (WR). The white rectangle in the inset map denotes the study area. The global distribution of the events used in this study is shown on the map in the top left corner. The events are located within the epicentral distance range 85° - 140° .

Figure 2. a) Map showing splitting parameters of single XKS waveforms. The non-null splitting parameters are shown with red bars oriented in the fast direction with length proportional to the delay time. The thin black arrows indicate backazimuth of phases giving null splitting measurements. b) 1-layer parameters obtained from joint-splitting analysis of XKS waveforms for each station. The red bars are oriented in the fast polarization direction with length proportional to the delay time. The main geological units in northwestern Namibia (after Konopásek et al., 2005) are also schematically depicted on the topography map.

Figure 3. Map showing the joint splitting parameters of this study (red bars), and the mean splitting parameters from the previous studies in Africa (blue bars; see Barruol. et al., 2009). The

bars are oriented in the fast polarization direction with length proportional to the delay time. The two plain arrows indicate the absolute motion vector of the African Plate in a No-Net-Rotation reference frame (Kreemer, et al., 2014).

Acknowledgments

We thank GEOFON data repository of Deutsches Geoforschungszentrum Potsdam (GFZ) for providing data from the temporary seismic networks XC and 6A, and the IRIS Data Management Center for the data from the permanent station TSUM (Albuquerque Seismological Laboratory/USGS, 2014, Global Seismograph Network (GSN - IRIS/USGS) [Data set]. International Federation of Digital Seismograph Networks. <https://doi.org/10.7914/SN/IU>).

Open Research

Data:

Data from the networks XC and 6A are accessible from GEOFON/GFZ via the following links:

XC: <https://doi.org/10.14470/KP6443475642>

6A: <https://doi.org/10.14470/1N134371>

Station TSUM belongs to the Global Seismograph Network (code IU, doi:

<https://doi.org/10.7914/SN/IU>).

Software:

The data analysis was performed using the MATLAB code SplitRacer. The code is available via the link: <https://www.geophysik.uni-frankfurt.de/64002762/Software>

Graphs:

The figures presented in the paper were generated using the analysis code (SplitRacer) and PyGMT (<https://www.pygmt.org>).

References

- Barruol, G., & Fontaine, F. R. (2013). Mantle flow beneath La Réunion hotspot track from SKS splitting. *Earth and Planetary Science Letters*, Elsevier, 2013, pp.108-121, doi: 10.1016/j.epsl.2012.11.017.
- Barruol, G., & Ismail, W.B. (2001). Upper mantle anisotropy beneath the African IRIS and Geoscope stations. *Geophysical Journal International*, 146(2), 549-561. doi: <https://doi.org/10.1046/j.0956-540x.2001.01481.x>.
- Barruol, G., Souriau, A., Vauchez, A., Diaz, J., Gallart, J., Tubia, J., & Cuevas, J. (1998). Lithospheric anisotropy beneath the Pyrenees from shear wave splitting, *J. geophys. Res.*, 103, 30 039-30 054. doi: <https://doi.org/10.1029/98JB02790>.
- Barruol, G., Wuestefeld, A., & Bokermann, G. (2009). SKS-Splitting Database. Université de Montpellier, Laboratoire Géosciences.
- Begg, G.C., Griffin, W.L., Natapov, L.M., O'Reilly, S.Y., Grand, S.P., O'Neill, C.J., Hronsky, J.M.A., Djomani, Y.P., Swain, C.J., Deen, T., & Bowden, P. (2009). The lithospheric architecture of Africa: Seismic tomography, mantle petrology, and tectonic evolution. *Geosphere*, 5(1), 23-50. doi: <https://doi.org/10.1130/GES00179.1>.
- Brune, S., Popov, A.A., & Sobolev, S.V. (2013). Quantifying the thermo-mechanical impact of plume arrival on continental breakup. *Tectonophysics*, 604, 51-59. doi: <https://doi.org/10.1016/j.tecto.2013.02.009>.
- Brune, S., Williams, S.E., Butterworth, N.P., & Müller, R.D. (2016). Abrupt plate accelerations shape rifted continental margins. *Nature*, 536(7615), 201-204. doi: <https://doi.org/10.1038/nature18319>.
- Celli, N.L., Lebedev, S., Schaeffer, A.J., Ravenna, M., & Gaina, C. (2020). The upper mantle beneath the South Atlantic Ocean, South America and Africa from waveform tomography with massive data sets. *Geophysical Journal International*, 221(1), 178-204. doi: <https://doi.org/10.1093/gji/ggz574>.
- Collins, J. A., Wolfe, C. J., & Laske, G. (2012). Shear wave splitting at the Hawaiian hot spot from the PLUME land and ocean bottom seismometer deployments, *Geochem. Geophys. Geosyst.*, 13, Q02007, doi:10.1029/2011GC003881.
- De Wit, M.J., Stankiewicz, J., & Reeves, C. (2008). Restoring Pan-African-Brasiliano connections: more Gondwana control, less trans-Atlantic corruption. *Geological Society, London, Special Publications*, 294(1), 399-412. doi: <https://doi.org/10.1144/SP294.20>.
- Druken, K. A., Kincaid, C., & Griffiths, R. W. (2013). Directions of seismic anisotropy in laboratory models of mantle plumes, *Geophys. Res. Lett.*, 40, 3544– 3549, doi:10.1002/grl.50671.
- Foster, D.A., Goscombe, B.D., & Gray, D.R. (2009). Rapid exhumation of deep crust in an obliquely convergent orogen: The Kaoko Belt of the Damara Orogen. *Tectonics*, 28(4). doi: <https://doi.org/10.1029/2008TC002317>.
- Fromm, T., Jokat, W., & Behrmann, J.H. (2017a). Interaction between a hotspot and a fracture zone: The crustal structure of Walvis Ridge at 6° E. *Tectonophysics*, 716, 108-120. doi: <https://doi.org/10.1016/j.tecto.2017.03.001>.
- Fromm, T., Jokat, W., Ryberg, T., Behrmann, J.H., Haberland, C., & Weber, M. (2017b). The onset of Walvis Ridge: Plume influence at the continental margin. *Tectonophysics*, 716, 90-107. doi: <https://doi.org/10.1016/j.tecto.2017.03.011>.
- Fromm, T., Planert, L., Jokat, W., Ryberg, T., Behrmann, J.H., Weber, M.H., & Haberland, C. (2015). South Atlantic opening: A plume-induced breakup?. *Geology*, 43(10), pp.931-934. doi: <https://doi.org/10.1130/G36936.1>
- Gibson, S.A., Thompson, R.N., Day, J.A., Humphris, S.E., & Dickin, A.P. (2005). Melt-generation processes associated with the Tristan mantle plume: Constraints on the origin of EM-1. *Earth and Planetary Science Letters*, 237(3-4), 744-767. doi: <https://doi.org/10.1016/j.epsl.2005.06.015>.

- 1 Goscombe, B., Hand, M., & Gray, D. (2003). Structure of the Kaoko Belt, Namibia: progressive
2 evolution of a classic transpressional orogen. *Journal of Structural Geology*, 25(7), 1049-1081.
3 doi: [https://doi.org/10.1016/S0191-8141\(02\)00150-5](https://doi.org/10.1016/S0191-8141(02)00150-5).
- 4 Hadiouche, O., Jobert, N., & Montagner, J.P. (1989). Anisotropy of the African continent inferred from
5 surface waves. *Physics of the earth and planetary interiors*, 58(1), 61-81. doi:
6 [https://doi.org/10.1016/0031-9201\(89\)90096-4](https://doi.org/10.1016/0031-9201(89)90096-4).
- 7 Hartog, R., & Schwartz, S.Y. (2000). Subduction-induced strain in the upper mantle east of the
8 Mendocino Triple Junction, California. *Journal of Geophysical Research: Solid Earth*, 105(B4),
9 7909-7930. doi: <https://doi.org/10.1029/1999JB900422>.
- 10 Heine, C., Zoethout, J., & Müller, R.D. (2013). Kinematics of the South Atlantic rift. *Solid Earth*, 4(2),
11 215-253. doi: <https://doi.org/10.5194/se-4-215-2013>, 2013.
- 12 Heit, B., Yuan, X., Jokat, W., Weber, M., & Geissler, W. (2010). WALPASS network, Namibia,
13 2010/2012. doi:10.14470/1N134371.
- 14 Heit, B., Yuan, X., Weber, M., Geissler, W., Jokat, W., Lushetile, B., & Hoffmann, K.H. (2015). Crustal
15 thickness and Vp/Vs ratio in NW Namibia from receiver functions: Evidence for magmatic
16 underplating due to mantle plume-crust interaction. *Geophysical Research Letters*, 42(9), 3330-
17 3337. doi: <https://doi.org/10.1002/2015GL063704>.
- 18 Hu, J., Liu, L., Faccenda, M., Zhou, Q., Fischer, K.M., Marshak, S., & Lundstrom, C. (2018).
19 Modification of the Western Gondwana craton by plume-lithosphere interaction. *Nature*
20 *Geoscience*, 11(3), 203-210. doi: <https://doi.org/10.1038/S31561-018-0064-1>.
- 21 Ito, G., Dunn, R., Li, A., Wolfe, C. J., Gallego, A., & Fu, Y. (2014), Seismic anisotropy and shear wave
22 splitting associated with mantle plume-plate interaction, *J. Geophys. Res. Solid Earth*, 119, 4923-
23 4937, doi:10.1002/2013JB010735.
- 24 Ito, G., Dunn, R., & Li, A. (2015). The origin of shear wave splitting beneath Iceland, *Geophysical*
25 *Journal International*, Volume 201, Issue 3, Pages 1297–1312, doi:
26 <https://doi.org/10.1093/gji/ggv078>.
- 27 Kind, R. (2000). Namibia. GFZ Data Services. doi:10.14470/KP6443475642.
- 28 Konopásek, J., Kröner, S., Kitt, S.L., Passchier, C.W., & Kröner, A. (2005). Oblique collision and
29 evolution of large-scale transcurrent shear zones in the Kaoko belt, NW Namibia. *Precambrian*
30 *Research*, 136(2), 139-157. doi: <https://doi.org/10.1016/j.precamres.2004.10.005>.
- 31 Kreemer, C., Blewitt, G., and Klein, E. C. (2014), A geodetic plate motion and Global Strain Rate Model,
32 *Geochem. Geophys. Geosyst.*, 15, 3849– 3889, doi:10.1002/2014GC005407.
- 33 Long, M. D., & Silver, P. G. (2009). Shear wave splitting and mantle anisotropy: measurements,
34 interpretations, and new directions, *Surv. Geophys.*, 30, 407-461, doi:
35 <https://doi.org/10.1007/s10712-009-9075-1>
- 36 Mainprice, D., Barruol, G., & Ben Ismail, W. (2000). The seismic anisotropy of the Earth's mantle: from
37 single crystal to polycrystal, in *Earth's Deep Interior: Mineral Physics and Tomography from the*
38 *Atomic to the Global Scale*, 237-264, ed. Karato, S.I., AGU, Washington, DC.
- 39 Moulin, M., Aslanian, D., & Unternehr, P. (2010). A new starting point for the South and Equatorial
40 Atlantic Ocean. *Earth-Science Reviews*, 98(1-2), 1-37. doi:
41 <https://doi.org/10.1016/j.earscirev.2009.08.001>.
- 42 Nicolas, A., & Christensen, N.I. (1987). Formation of anisotropy in upper mantle peridotites—a review,
43 in *Composition, Structure and Dynamics of the Lithosphere-Asthenosphere System*, 16, 111-123.
44 doi: <https://doi.org/10.1029/GD016p0111>.
- 45 Pandey, S., Yuan, X., Debayle, E., Geissler, W.H. & Heit, B. (2022). Plume-lithosphere interaction
46 beneath southwestern Africa—Insights from multi-mode Rayleigh wave tomography.
47 *Tectonophysics*, 229587. doi: <https://doi.org/10.1016/j.tecto.2022.229587>.

- 1 Planert, L., Behrmann, J., Jokat, W., Fromm, T., Ryberg, T., Weber, M., & Haberland, C. (2017). The
2 wide-angle seismic image of a complex rifted margin, offshore North Namibia: Implications for
3 the tectonics of continental breakup. *Tectonophysics*, 716, 130-148. doi:
4 <https://doi.org/10.1016/j.tecto.2016.06.024>.
- 5 Renne, P. R., Ernesto, M., Pacca, I. G., Coe, R. S., Glen, J., Prevot, M., & Perrin, M. (1992). The age of
6 Parana flood volcanism, rifting of Gondwanaland, and the Jurassic-Cretaceous boundary:
7 *Science*, v. 258, 975-979, doi: 10.1126/science.258.5084.975
- 8 Renne, P.R., Glen, J.M., Milner, S.C., & Duncan, A.R. (1996). Age of Etendeka flood volcanism and
9 associated intrusions in southwestern Africa. *Geology*, v. 24, 659-662, doi: 10.1130 /0091 -
10 7613(1996)024<0659:AOEFVA>2.3.CO;2.
- 11 Reiss, M.C., & Rumpker, G. (2017). SplitRacer: MATLAB code and GUI for semiautomated analysis
12 and interpretation of teleseismic shear-wave splitting. *Seismological Research Letters*, 88(2A),
13 392-409. doi: <https://doi.org/10.1785/0220160191>
- 14 Richards, M. A., Duncan, R. A., & Courtillot, V. E. (1989). Flood basalts and hot-spot tracks: Plume
15 heads and tails, *Science*, 246, 103-107, doi: 10.1126/science.246.4926.10
- 16 Rumpker, G., & Ryberg, T. (2000). New “Fresnel-zone” estimates for shear-wave splitting observations
17 from finite-difference modeling. *Geophysical Research Letters*, 27(13), 2005-2008. doi:
18 <https://doi.org/10.1029/2000GL011423>.
- 19 Rumpker, G., & Silver, P.G. (1998). Apparent shear-wave splitting parameters in the presence of
20 vertically varying anisotropy. *Geophysical Journal International*, 135(3), 790-800. doi:
21 <https://doi.org/10.1046/j.1365-246X.1998.00660.x>.
- 22 Ryberg, T., Haberland, C., Haberau, T., Weber, M.H., Bauer, K., Behrmann, J.H., & Jokat, W. (2015).
23 Crustal structure of northwest Namibia: Evidence for plume-rift-continent interaction. *Geology*,
24 43(8), 739-742. doi: <https://doi.org/10.1130/G36768.1>.
- 25 Savage, M. K. (1999). Seismic anisotropy and mantle deformation: What have we learned from shear
26 wave splitting?, *Rev. Geophys.*, 37, 65- 106, doi:10.1029/98RG02075.
- 27 Silver, P.G. (1996). Seismic anisotropy beneath the continents, Probing the depths of geology, *Ann. Rev.*
28 *Earth planet. Sci.*, 24, 385-432.
- 29 Silver, P.G., & Chan, W.W. (1991). Shear wave splitting and subcontinental mantle deformation, *J.*
30 *geophys. Res.*, 96, 16 429-16 454. doi: <https://doi.org/10.1029/91JB00899>.
- 31 Silver, P.G., & Savage, M.K. (1994). The interpretation of shear-wave splitting parameters in the
32 presence of two anisotropic layers. *Geophysical Journal International*, 119(3), 949-963. doi:
33 <https://doi.org/10.1111/j.1365-246X.1994.tb04027.x>.
- 34 Ussami, N., Chaves, C.A.M., Marques, L.S., & Ernesto, M. (2013). Origin of the Rio Grande Rise-Walvis
35 Ridge reviewed integrating palaeogeographic reconstruction, isotope geochemistry and flexural
36 modelling. *Geological Society, London, Special Publications*, 369(1), 129-146. doi:
37 <https://doi.org/10.1144/SP369.10>.
- 38 Vauchez, A., Tommasi, A., Barruol, G., & Maumus, J. (2000). Upper mantle deformation and seismic
39 anisotropy in continental rifts, *Phys. Chem. Earth*, 25, 111-117. doi:
40 [https://doi.org/10.1016/S1464-1895\(00\)00019-3](https://doi.org/10.1016/S1464-1895(00)00019-3).
- 41 Walker, K. T., Bokelmann, G. H. R., & Klemperer, S. L. (2001). Shear-wave splitting to test mantle
42 deformation models around Hawaii, *Geophys. Res. Lett.*, 28, 4319– 4322,
43 doi:10.1029/2001GL013299.
- 44 Walker, K. T., Bokelmann, G. H. R., & Klemperer, S. L. (2005). Shear-wave splitting around the Eifel
45 hotspot: evidence for a mantle upwelling, *Geophysical Journal International*, Volume 163, Issue
46 3, 962–980, doi: <https://doi.org/10.1111/j.1365-246X.2005.02636.x>.

- 1 Wilson, M. (1992). Magmatism and continental rifting during the opening of the South Atlantic Ocean: a
2 consequence of Lower Cretaceous super-plume activity? Geological Society, London, Special
3 Publications, 68(1), 241-255. doi: <https://doi.org/10.1144/GSL.SP.1992.068.01.15>.
- 4 Yuan, X., Heit, B., Brune, S., Steinberger, B., Geissler, W.H., Jokat, W., & Weber, M. (2017). Seismic
5 structure of the lithosphere beneath NW Namibia: Impact of the Tristan da Cunha mantle plume.
6 Geochemistry, Geophysics, Geosystems, 18(1), 125-141. doi:
7 <https://doi.org/10.1002/2016GC006645>.

1 **Figures**

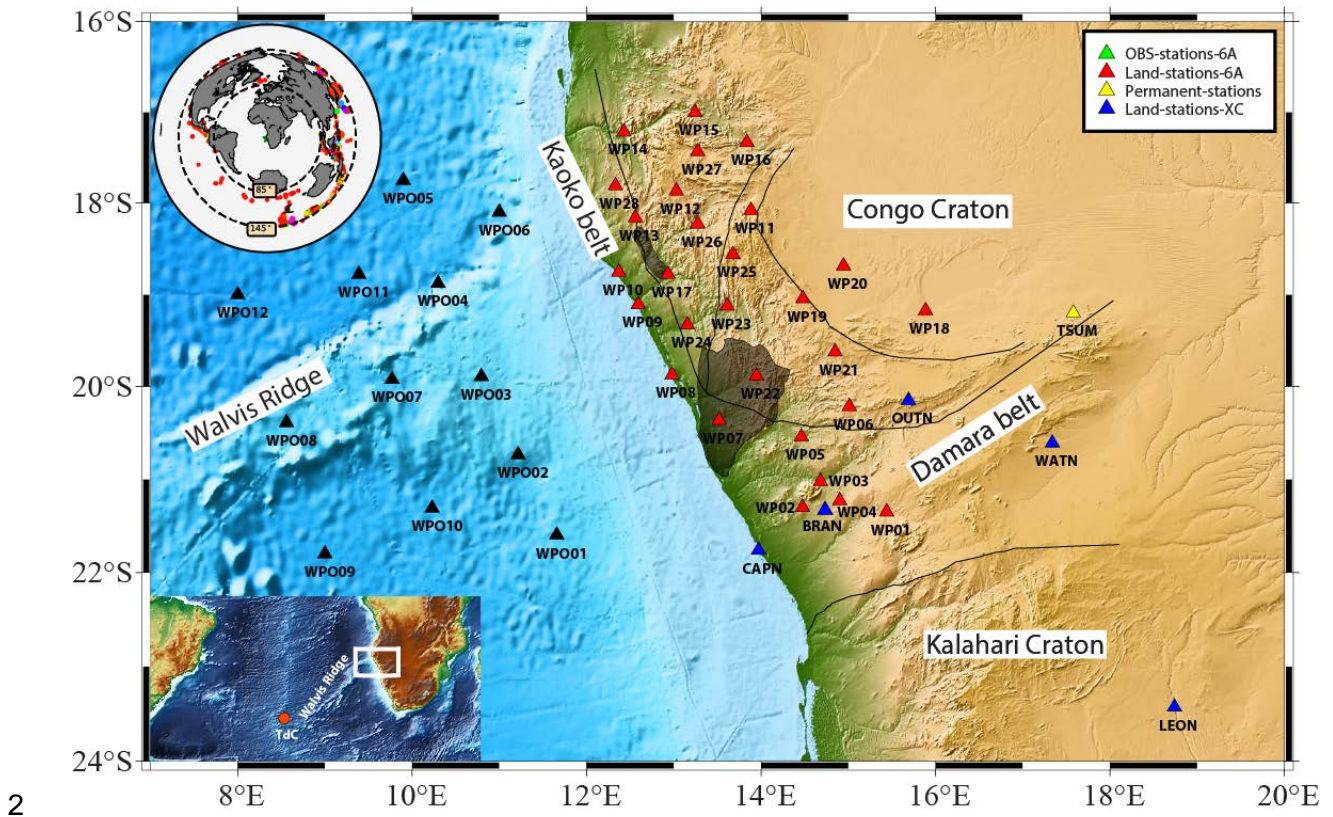


Figure 1

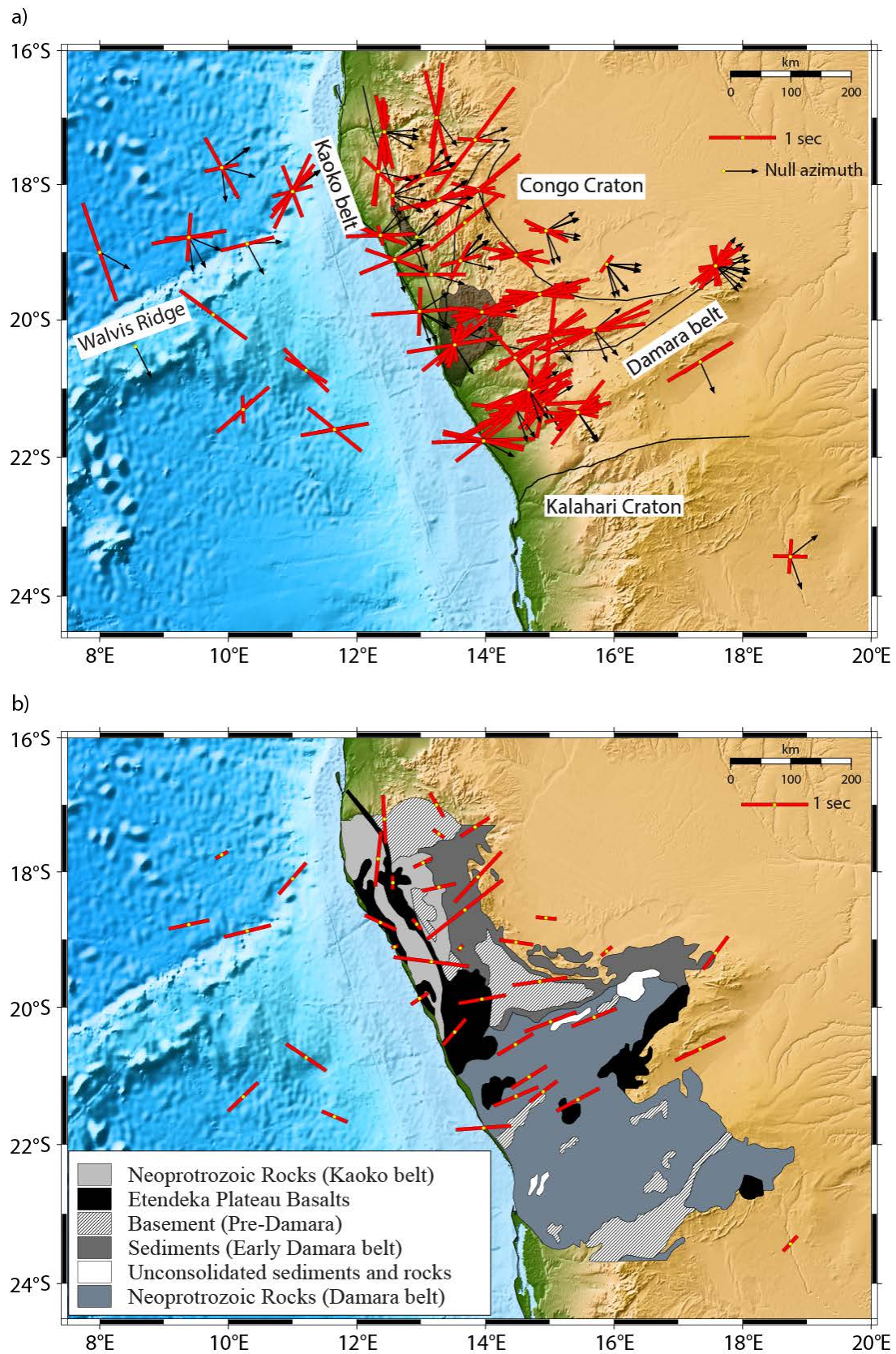


Figure 2

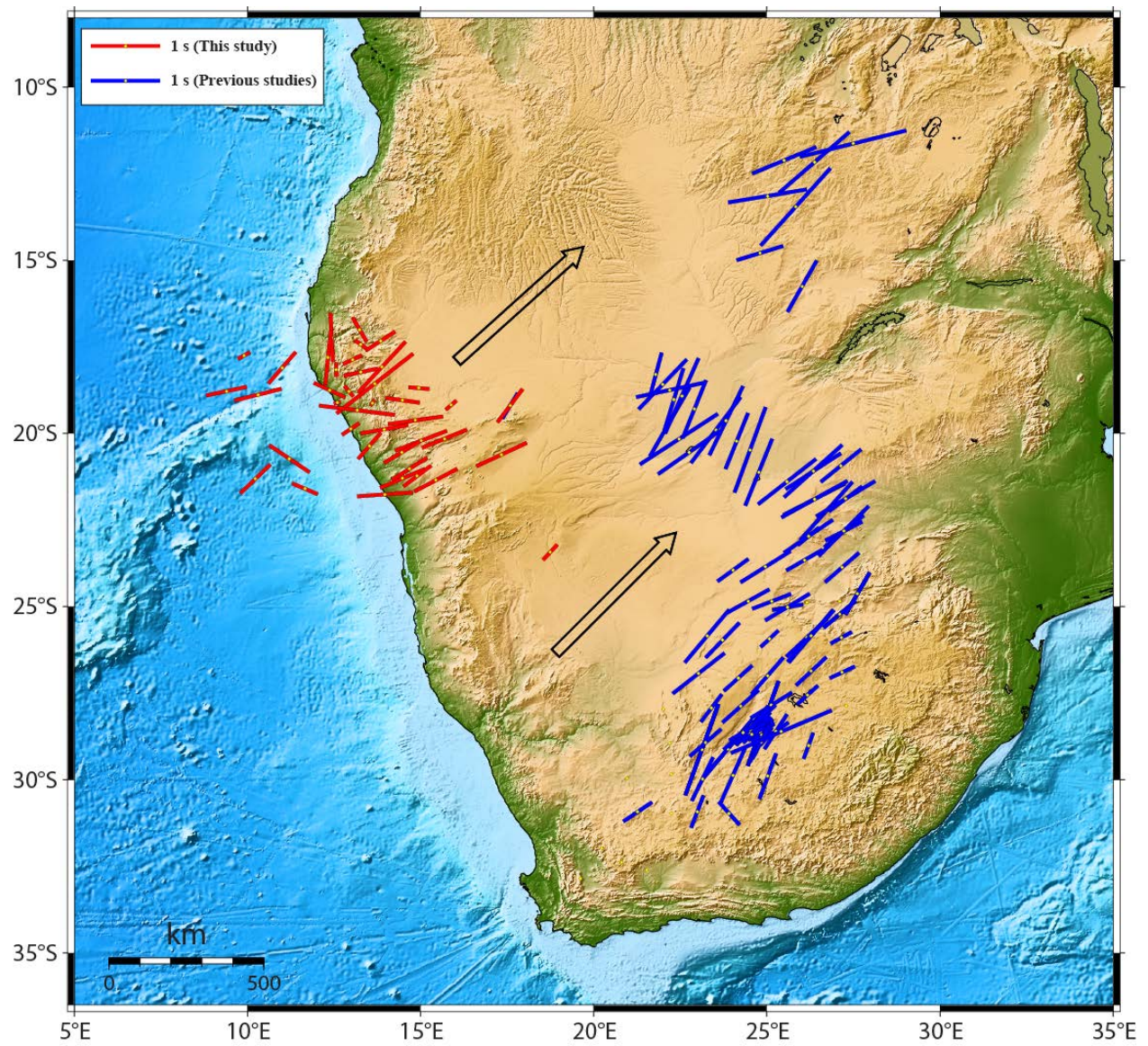


Figure 3